Journal of Drug Delivery Science and Technology 99 (2024) 105929

Contents lists available at ScienceDirect

Journal of Drug Delivery Science and Technology

journal homepage: www.elsevier.com/locate/jddst

Lactobacilli cell-free supernatants: Potential green and natural enhancers for nose-to-brain delivery of small hydrophilic molecules

Elisa Corazza [a,1], Janik Martin [b,1], Barbara Giordani [a], Beatrice Vitali [a], Martina Rossi [a,c], Angela Abruzzo [a], Federica Bigucci [a], Teresa Cerchiara [a], Massimiliano Pio di Cagno [d], Barbara Luppi [a,*], Katharina Schindowski [b]

[a] Department of Pharmacy and Biotechnology, Alma Mater Studiorum, University of Bologna, Via San Donato 19/2, 40127, Bologna, Italy
[b] Institute of Applied Biotechnology, University of Applied Science Biberach, Hubertus-Liebrecht Straße 35, 88400, Biberach, Germany
[c] Center for Applied Biomedical Research (CRBA), Alma Mater Studiorum, University of Bologna, Via Massarenti 9, 40126, Bologna, Italy
[d] Department of Pharmacy, Faculty of Mathematics and Natural Sciences, University of Oslo, Sem Sælands vei 3, 0371, Oslo, Norway

ARTICLE INFO

Keywords:
Nose-to-brain
Postbiotic
Lactobacillus
Sustainability
Diffusion
Enhancer

ABSTRACT

Concerns about environmental health are driving pharmaceutical industries towards more eco-friendly and biocompatible products. Lactobacilli cell-free supernatants (CFS) are mixtures of soluble factors derived from the microbial growth of beneficial bacteria with the potential to serve as natural and sustainable excipients in emerging formulations. This work aims to verify the usefulness of the CFS obtained from human *L. crispatus* BC5, *L. gasseri* BC9 and BC12 as enhancers in the nose-to-brain absorption of small hydrophilic molecules. CFS influence on cell viability was investigated together with their ability to increase the diffusion of sodium fluorescein across *in vitro* models of the olfactory epithelium. The enhancing mechanism was studied through differential scanning calorimetry analysis and immunostaining assay of zonula occludens-1. The use of 25 % (v/v) of all lactobacilli CFS on porcine olfactory epithelial primary cells was not associated with any cytotoxic effect, but only the CFS obtained from BC5 was pointed out as a permeation enhancer across both the biomimetic membrane PermeaPad®, the porcine olfactory tissue, and the primary cell model. The enhancing mechanism seems to rely on the CFS perturbation effect on lipid membranes that, in the case of the cell-based model, probably also results in an alteration of tight junctions' activity.

1. Introduction

Because of their carbon footprint and toxicological impact on organisms and environmental health, pharmaceuticals are regarded as emerging pollutants [1]. Therefore, policy initiatives are going in the direction of shifting the paradigm: the focus should not be exclusively on the standard of bioactive compounds, but a broader look that also includes the nature of excipients as well as the entire production process should be adopted, thus ending up with a pharmaceutical product that is less detrimental to the environment [2,3].

Recently, the application of postbiotics mixtures and individual postbiotics in food and pharmaceutical industries has been reviewed [4]. These can be defined as biological materials containing soluble probiotic-derived metabolites or cell wall-derived components without the presence of viable microorganisms [5]. Examples of postbiotics are cell-free supernatants (CFS), which represent the mixture of metabolites that bacteria secrete in the culture medium during fermentation [6] and that are well established for their beneficial effect on human health [5]. Regardless of being exploited as therapeutic agents, little is known concerning their employment as excipients, even though the presence of organic acids and short-chain fatty acids within their complex composition [5,6] suggests a potential application as pharmaceutical aids to improve bioavailability of drugs. Demonstrating this alternative use of CFS would answer the demand for more eco-friendly products. Indeed, CFS are natural compounds, thus are suggested to feature greater biocompatibility than synthetic substances [3,7], and

* Corresponding author.
E-mail addresses: elisa.corazza7@unibo.it (E. Corazza), martin@hochschule-bc.de (J. Martin), barbara.giordani4@unibo.it (B. Giordani), b.vitali@unibo.it (B. Vitali), martina.rossi12@unibo.it (M. Rossi), angela.abruzzo2@unibo.it (A. Abruzzo), federica.bigucci@unibo.it (F. Bigucci), teresa.cerchiara2@unibo.it (T. Cerchiara), m.p.d.cagno@farmasi.uio.no (M.P. di Cagno), barbara.luppi@unibo.it (B. Luppi), schindowski@hochschule-bc.de (K. Schindowski).
[1] These authors contributed equally to this work.

https://doi.org/10.1016/j.jddst.2024.105929
Received 1 March 2024; Received in revised form 27 June 2024; Accepted 28 June 2024
Available online 3 July 2024

postbiotic-producing cells can be cultivated using waste substrates derived from agricultural and industrial activities, hence supporting sustainability [8].

The intranasal route appears as a valid delivery strategy for an increasing number of drugs targeting the brain, particularly for those indicated for acute and rapid treatment of neurologic conditions [9]. Despite the growing interest in exploring nose-to-brain delivery as a potential alternative method for administering therapeutics, some formulation constraints remain [10]; among others, the less efficient absorption of hydrophilic and/or high molecular weight molecules compared to small lipophilic drugs [10,11]. Nonetheless, the trans-epithelial passage of low liposoluble drugs can be improved by using permeation enhancers, which are excipients bearing the ability to modulate membrane structures and/or tight junctions [10].

As the success of a formulation is closely related to the active ingredient's ability to cross the biological barriers it encounters, digging into the enhancing properties of innovative pharmaceutical aids is of paramount importance [12]. When it comes to the early stages of drug development, excised tissues, cell monolayers, and artificial membranes are useful *in vitro* tools to assess membrane permeability, even though each one shows its pros and cons [13]. *Ex vivo* models, specifically those of animal origin, are easily accessible from slaughterhouses and preserve both the structure and composition of the anatomical region from where they were sourced. However, they must be handled within a short post-mortem delay, the isolation process is usually extremely labor-intensive, and they frequently show interindividual differences [14]. Alternatively, different cell lines can be employed to study drug permeation across cell monolayers that resemble the function and morphology of the nasal epithelium, even though this often requires 21 days of *in vitro* cell differentiation [13]. Usually, tumor cell lines are preferred over primary cell models as they are permanent cells, can be easily cultured, and are associated with higher reproducibility, but feature a reduced differentiative capacity [14]. Even though cell-based assays allow for moderate throughput, cell-free biomimetic models are more suitable for routine and screening procedures, they enable the measurements of the passive permeability of compounds cost-effectively, but they are not as physiologically relevant as the *ex vivo* and cell-based models [12]. Being made of lipids soaked in a filter (Nasal-Parallel artificial membrane permeability assay [15]) or enclosed in support membranes (PermeaPad® [16]), they cannot account for relevant interactions that occur in biological systems [17].

Since it has been demonstrated that the biosurfactant, an example of cell-bound metabolite produced by the human *Lactobacillus gasseri* BC9, might be employed as a natural enhancer for hydrocortisone intranasal permeation [18], our question was whether the complex mixture of products derived from the microbial metabolism could itself affect drug absorption. We answered this question by proving the ability of the CFS produced by the human *L. crispatus* BC5 (BC5-CFS), *L. gasseri* BC9 (BC9-CFS), and *L. gasseri* BC12 (BC12-CFS) to improve the nose-to-brain absorption of fluorescein sodium salt, a small hydrophilic paracellular marker, across a cell-free, a tissue-based and a cell-based model of the olfactory mucosa. Besides, to elucidate the mechanism of action of these potential innovative excipients, differential scanning calorimetry analysis of the treated nasal tissue and immunostaining assay of the tight junction protein zonula occludens-1 were performed.

2. Material and methods

2.1. Materials

Fluorescein sodium salt (FSS), sodium chloride (NaCl), and sodium hydroxide (NaOH) were purchased from Sigma-Aldrich (Taufkirchen, Germany). In contrast, phosphate buffer saline pH 7.4 (ROTI®Fair PBS pH 7.4 1000 mL/tablet) and Octenisept® were bought from Carl Roth (Karlsruhe, Germany) and Schülke & Mayr GmbH (Norderstedt, Germany), respectively. Regarding the microbiological part, Man, Rogosa, and Sharpe (MRS) culture medium was supplied by Difco (Detroit, USA) and L-cysteine hydrochloride monohydrate by Merck (Darmstadt, Germany). Concerning cell culturing and biological assays, Dulbecco's Modified Eagle Medium: Nutrient Mixture F12 (DMEM – F12) w/o L-Glutamine w/o HEPES w/o Glucose, Earle's balanced salt solution (EBSS), Minimum essential medium (MEM) w/o phenol red, MEM non-essential amino acids (NEAA) were provided by Gibco (Darmstadt, Germany). The antibiotics gentamycin sulfate and kanamycin sulfate were supplied by Carl Roth (Karlsruhe, Germany), while Penicillin/Streptomycin (PenStrep) (10,000 U) was obtained from AppliChem (Darmstadt, Germany). Besides, L-Glutamine (Gln), Fetal Bovine Serum (FBS), debris removal solution, rat tail collagen solution, and AlamarBlue™ HS Cell Viability Reagent Invitrogen were purchased from Gibco (Darmstadt, Germany), Capricorn Scientific (Ebsdorfergrund, Germany), Milteny Biotec (Bergisch Gladbach, Germany), Primacyte (Schwerin, Germany), and Thermo Fisher Scientific (Darmstadt, Germany), respectively. Lastly, the pronase was delivered by Sigma-Aldrich (Taufkirchen, Germany), and the antimycotic amphotericin B was provided by Carl Roth (Karlsruhe, Germany). Methanol, acetone, piperazine-N-N′-bis(2-ethanesulphonic acid) (PIPES), ethylene glycol-bis(2-aminoethylether)-N,N,N,N-tetraacetic acid (EGTA), Tween-20, and bovine serum albumin (BSA) were used for immunofluorescence staining and were purchased from Carl Roth (Karlsruhe, Germany). Magnesium chloride hexahydrate ($MgCl_2 \times 6H_2O$) and ammonium chloride (NH_4Cl) were delivered by Merck (Darmstadt, Germany). 4′,6-diamidino-2-phenylindole (DAPI) was obtained from Sigma-Aldrich (Taufkirchen, Germany). For embedding of stained transwells mowiol and 1,4 diazabicyclo[2.2.2]octane (DABCO) were purchased from Sigma-Aldrich (Taufkirchen, Germany), whereas glycerol and tris-(hydroxymethyl)-amino methane (TRIS) were purchased from Carl Roth (Karlsruhe, Germany). Hereafter the compositions of the different cultivation media and buffers are described (Table 1).

2.2. Cell-free supernatant isolation and pH adjustment

The cell-free supernatants (CFS) were obtained from the human *L. crispatus* BC5 (BC5-CFS), *L. gasseri* BC9 (BC9-CFS), and *L. gasseri* BC12 (BC12-CFS), cultured in MRS broth supplemented with 0.05 % L-cysteine at 37 °C in anaerobic jars containing Gas-Pak EZ (Beckton, Dickinson and Co., Milan, Italy) [19]. Briefly, overnight lactobacilli cultures were used to inoculate 90 mL of MRS broth at a concentration of 10^6 CFU/mL and allowed to grow for 24 h. After this incubation, bacterial cells were precipitated by centrifugation (10,000×*g* for 10 min) (Centrisart G-16C; Sartorius, Göttingen, Germany) and the supernatants were recovered.

Table 1
Composition of the different employed media and buffers.

Medium/Buffer	Composition
Pronase medium	EBSS - 1.4 mg/mL pronase - 1:100 PenStrep - 1:100 Gentamycin sulfate - 1:100 kanamycin sulfate - 1:10,000 amphotericin B
Primary culture adhesion medium	DMEM: F12 (1:1) – 20 % FBS – 2 mM Gln – 1 % NEAA – 4.5 g/L Glucose – 1:500 PenStrep – 1:100 gentamycin sulfate – 1:100 kanamycin sulfate – 1:10,000 amphotericin B
Primary culture medium	DMEM: F12 (1:1) – 10 % FBS – 2 mM Gln – 1 % NEAA – 4.5 g/L Glucose – 1:500 PenStrep – 1:100 gentamycin sulfate – 1:100 kanamycin sulfate – 1:10,000 amphotericin B
PEM	80 mM PIPES – 5 mM EGTA – 1 mM $MgCl_2$ – 18.5 ml 10 M NaOH – 800 ml H_2O Adjust pH to 7.4 with NaOH and set volume to 1 L with H_2O
PEMT	PEM – 0.2 % Tween-20
Quenching buffer	PEM – 50 mM NH_4Cl
Blocking/staining buffer	PEMT – 0.5 % BSA
Mowiol embedding medium	60 g mowiol – 150 g glycerol – 300 ml 0.2 M TRIS (pH 8.5) – 2.5 % DABCO in H_2O

The latter were subjected to pH measurement (Basic 20 pH meter, Crison Strumenti Spa, Modena, Italy) and adjusted to a pH value of 6 by using NaOH 10 % (w/v). Finally, the lactobacilli supernatants were filtered with a polyethersulfone (PES) vacuum filtration unit 0.22 μm pore size (Sartolab®, Sartorius, Goettingen, Germany) to obtain the CFS and to ensure sterility.

2.3. Cell culture

2.3.1. Olfactory epithelial primary cell isolation

Olfactory epithelial primary cells (OEPC) were isolated from mucosal explants derived from the olfactory region of 4 – 6-month-old slaughterhouse pigs (Metzgerei Joas, Dietenheim, Germany). Tissues were handled within 1.5 h from slaughtering and according to the protocol described by Ladel and co-workers but with slight modifications [20]. The mucosa explants excised from the *regio olfactoria* were disinfected using Octenisept® and washed twice with PBS pH 7.4. The epithelial cells were isolated by incubation for 1 h at 37 °C with pronase medium in a T25 cell-suspension cultivation flask (Cellstar®, Greiner bio-one GmbH, Frickenhausen, Germany). The resulting suspension was collected and centrifuged at 300×*g* for 10 min at 4 °C (Heraeus 4 KR centrifuge, Thermo Scientific). The supernatant was removed and the cell pellet was resuspended in cold PBS and processed for debris removal according to the manufacturer protocol. Lastly, cells were resuspended in appropriate volumes of primary culture adhesion medium and directly seeded in cell culture inserts.

2.3.2. Cells seeding and cultivation in air-liquid interface conditions

OEPC were seeded in cell culture inserts (ThinCert™ 24 well polyethylene terephthalate 1 μm, Greiner Bio-one, Frickenhausen, Germany), previously coated with 0.05 mg/mL rat tail collagen solution for 48 h at 37 °C. Cells were seeded at a density of ~10^6 cells/mL and cultivated submerged at standard conditions (37 °C, 5 % CO_2, 96 % rH) for one day. After 24 h, the apical medium was removed to cultivate cells under ALI (air-liquid interface) conditions for 21 days and the basolateral medium was changed to the primary culture medium. The exchange was necessary to contain fibroblast growth due to reduced serum concentration. Cells were apically washed with 200 μL PBS and the medium (260 μL/well) was changed every two days.

2.4. Cell viability assay

After 21 days of cultivation in ALI conditions, cells were washed with 200 μL PBS, and inserts were moved to a new 24-well plate, which had been previously filled with 260 μL/well of MEM w/o phenol red. CFS's and MRS's cytotoxic effect was investigated at three different volume ratios, 12.5 %, 25 %, and 50 % (v/v). Specifically, cells were treated with 100 μL volume, half of which was represented by the medium and the other half was distributed between MRS or the investigated CFS and normal saline solution (NaCl 0.9 % w/v), which was used as diluent. MEM was employed as the negative control (CTRL-), whereas DMSO 50 % (v/v) as the positive control (CTRL+). Plates were stored in the incubator at standard conditions for 24 h. Afterward, treatment solutions were removed and 100 μL/well of AlamarBlue™ HS Cell Viability Reagent diluted 1:10 in MEM w/o phenol red were added apically. Plates were stored in the incubator for 5 h before detecting the fluorescence signal at the fluorescence spectrophotometer (Infinite® 200 Pro, TECAN, Männedorf, Switzerland) using the following setup: plate shaking for 2 s in linear mode with an amplitude of 1 mm and a frequency of 886.9 rpm before the measurement, that was performed at excitation and emission wavelengths of 530 nm and 590 nm, respectively.

2.5. Osmolality measurement

As the osmolarity of the applied medium can influence permeability, the investigated CFS, as well as MRS, were tested for their osmolality values before trying out their potential permeation-enhancing effect. The osmolality (mOsm/kg) was measured through a cryoscopic osmometer (Osmomat 030, Gonotec, Berlin, Germany) calibrated with a reference solution of 300 mOsm/kg and MilliQ water as 0 mOsm/kg. The analysis was carried out on samples used at 25 % v/v in normal saline solution as it was the concentration employed during the following studies.

2.6. In vitro permeation studies

The role of the considered CFS as absorption enhancers was investigated by proving their ability to increase the apparent permeability of fluorescein sodium salt (FSS). Alongside, to obtain a more complete and reliable approach to figuring out their enhancing properties, diffusion studies were performed by combining three different *in vitro* models: the biomimetic membrane PermeaPad®, the excised porcine olfactory tissue, and the primary cell model (OEPC). Moreover, to ensure that the products of the lactobacilli metabolism were the only ones responsible for the improvement in the drug diffusion, two control samples were considered: the FSS solubilized in normal saline solution in the absence and presence of 25 % (v/v) of the lactobacilli culture medium, named as CTRL and MRS respectively.

2.6.1. Sample preparation

Samples were prepared by solubilizing FSS at the concentration of 0.67 mg/mL in normal saline solution and filtered with 0.22 μm PES syringe filters (Whatman ™ Puradisc 25 mm, Cytivia, Dassel, Germany) to ensure sterility, which was strictly necessary for the diffusion study across primary cells. For consistency, sterility was also maintained during transport experiments across the other two barriers. Lastly, the FSS solution was mixed with 25 % (v/v) of NaCl 0.9 % (w/v) for the CTRL sample, or MRS or one of the three CFS, having a final concentration of the paracellular marker equal to 0.5 mg/mL.

2.6.2. Biomimetic model

The ready-to-use biomimetic membrane PermeaPad® (Phabioc GmbH, Espelkamp, Germany) was mounted on Franz-type static glass vertical diffusion cells equipped with a V6A Stirrer (PermeGear Inc., Hellertown, PA, USA). The acceptor chamber was filled with 12 mL of MEM w/o phenol red supplemented with 10 % FBS (named transport or permeation medium), which was kept under stirring and at the temperature of 37 °C thanks to a surrounding jacket. 200 μL of test solution were loaded in the donor chamber and at predetermined time points (after 30, 60, 120, 180, 240, and 300 min) 200 μL were withdrawn from the sampling port and quickly replaced with an equal volume of permeation medium. Once the diffusion study was completed, the content of both the donor and acceptor compartments was collected, and the membrane was submerged with 2 mL of normal saline solution and then kept under stirring at room temperature for 3 h to release the FSS that eventually accumulated. This sample was then centrifuged at 12,000×*g* for 15 min (Microspin 12, Biosan, Riga, Latvia) to take apart debris from the supernatant containing FSS.

2.6.3. Tissue-based model

The porcine tissue was sourced from a local slaughterhouse (Salumificio Capelli, Bologna, Italy) and processed for the isolation of the nasal olfactory mucosa. The septum was excised, and the *regio olfactoria* was extracted from the nasal cavity using forceps and a scalpel. Subsequently, the mucosa was separated from the attached cartilaginous tissue and rinsed with a normal saline solution. The biological specimens were then preserved in aluminum foil at −20 °C until they were required for use.

The permeation study across the tissue-based model was performed following the procedure described for the biomimetic model (see Section 2.6.2), but before starting the experiment, the integrity of the mucosa

was verified. First, the excised nasal mucosa was clamped between the donor and acceptor compartments, with the latter being filled with 12 mL of NaCl 0.9 % (w/v). Then, the Franz cell was repeatedly tilted and the eventual accumulation of saline solution in the donor compartment due to the loss of membrane integrity was checked. Moreover, to ensure that the CFS did not damage the olfactory mucosa, at the beginning and the end of the diffusion study, the electrical resistance was measured (voltage: 100 mV, frequency: 100 Hz; Agilent 4263 B LCR Meter, Microlease, I). To do so, both the Franz cell's chambers were loaded with normal saline solution (12 mL for the acceptor and 1 mL for the donor) and each compartment was supplied with an electrode. Only mucosa specimens that did not appear to be leaky and were characterized by unchanged electrical resistance values between the starting and end points were included in the study.

2.6.4. Cell-based model

After 21 days in ALI cultivation mode, cells were washed apically with 200 μL/well of PBS pH 7.4 and then processed to ensure the integrity of the cell layer. The transepithelial electrical resistance (TEER) measurement was performed directly in the permeation medium by adding 500 μL and 350 μL of it to the basolateral and apical compartments of the transwell, respectively. Cells were left to equilibrate for 20 min at 37 °C and then cooled down at room temperature for 15 min. The TEER was measured employing an EVOM2 epithelial volt ohmmeter and chopstick electrodes (World Precision Instruments, USA). The instrument was calibrated with a control resistor (1000 Ω) and the resistance produced by an insert without cells was determined to serve as a blank. The TEER of each insert was measured in triplicate and the obtained values (already subtracted by the blank) were multiplied by the growth area of the membrane (0.336 cm^2). Because a previously published work pointed out a correlation between permeability and TEER for primary cells (higher TEER resulted in lower flux), only those cell layers exhibiting TEER values equal to or higher than 300 Ωcm^2 were included in the experiment [20]. The transport study was performed in the transwell setup by placing cell inserts in 260 μL of permeation medium and adding 100 μL of a sample (see Section 2.6.1 for sample preparation) to the apical compartment. FSS permeation was studied under atmospheric conditions, in a steady state, and over 5 h 20 μL were sampled from the basolateral compartment at the usual time points and they were immediately refilled with fresh permeation medium. At the end of the experiment, the apical and basolateral solutions were collected, the cell layer was washed with 200 μL of PBS, and the TEER measurement was repeated as previously described (only cell layers bearing a TEER $\geq$ 300 Ωcm^2 were considered). To calculate the mass balance at the end of the experiment, the support membrane was removed from the insert and placed in 200 μL of Milli-Q water. Subsequently, cells were subjected to three cycles of freeze-thawing (30 min at −80 °C followed by 30 min at 37 °C), and the obtained suspension was centrifuged at 12,000×*g* for 15 min to remove cell debris.

2.6.5. Marker quantification and calculations

FSS quantification in the different samples was achieved using the fluorescence spectrophotometer with the following setup: plate shaking for 3 s in linear mode with an amplitude of 1 mm and a frequency of 886.9 rpm before the measurement, that was performed at excitation and emission wavelengths of 460 nm and 512 nm, respectively.

The cumulative amount of drug permeating per unit area (μg/cm^2) versus time (min) was plotted and the slope of the linear portion of the plot was calculated as the flux j (μg/cm^2 min). The lag time was determined by intercepting the linear portion of the cumulative amount of drug permeated versus time with the abscissa. The apparent permeability coefficient (P_{app}) was determined using **Equation (1)**:

$$P_{app} = \frac{dM}{dt} \times \frac{1}{A \times C_0} \quad \text{Equation 1}$$

where dM/dt (μg/s) is the slope at the steady state period, A (cm^2) is the diffusion surface area and C_0 (μg/mL) is the initial drug concentration within samples. Besides, for a better understanding of the permeation-enhancing properties of the tested CFS, the enhancement ratio (ER) was calculated according to **Equation (2)**:

$$ER = \frac{P_{app}\ with\ CFS\ or\ MRS}{P_{app}\ CTRL} \quad \text{Equation 2}$$

2.7. Differential scanning calorimetry

Differential scanning calorimetry (DSC) analyses were carried out to investigate a potential interaction between the selected CFS and the lipid components of the olfactory nasal mucosa. The nasal mucosa explant was cut into 5 pieces weighing the same, which were then treated for 5 h with 3 mL of normal saline solution in the absence (CTRL) or presence of 25 % v/v of either MRS or one of the three CFS. Once the incubation time had expired, the tissue specimens were washed with MilliQ water and left to dry in a desiccator under vacuum containing $CaCl_2$ for 48 h. DSC analysis was conducted utilizing a PerkinElmer DSC 6 instrument (PerkinElmer, Beaconsfield, UK) with nitrogen employed as the purge gas at a flow rate of 20 mL/min. Samples, weighing between 2 and 3 mg, were loaded into an aluminum pan and subjected to a heating process, starting at 30 °C and ending at 180 °C, with a scanning rate of 10 °C/min.

2.8. Immunostaining assay of tight junctions

To evaluate the influence of the three CFS on the barrier integrity, immunofluorescence (IF) staining against the tight junction marker zonula occludens-1 (ZO-1) was performed. Therefore, the primary cells were treated as described in section 2.6.4. The only difference was that there was no sampling during the 5 h permeation. Further, after the last washing step with 200 μL PBS, the cells were fixated by adding 200 μL of a 1:1 methanol/acetone mixture to the apical and 500 μL to the basolateral compartment. Cells were placed at −20 °C for 20 min. Afterward, the mixture was removed and replaced with PBS. In PBS cells can be stored for up to 1 week at 4 °C until staining is performed. All washing steps were performed by applying 300 μL of the buffer to the apical and 500 μL to the basolateral compartment. Transwells were washed 3 times with PEMT for 5 min. Next, a 5 min washing step with quenching buffer was performed followed by another washing step with PEMT (twice for 5 min each). Afterward, each transwell was blocked by adding 200 μL blocking buffer to the apical compartment for 1 h at room temperature (RT) or overnight at 4 °C. After blocking, the blocking buffer was removed and 100 μL of a 1:100 dilution of anti-tight junction protein 1 antibody (Novus Biologicals, #NBP1-85047, Centennial, USA) in blocking buffer was applied overnight at 4 °C. Then, the primary antibody was removed and the transwells were washed 4 times for 5 min each using blocking buffer. In the end, 100 μL of a 1:300 dilution of the secondary antibody (F(ab')2 goat anti-rabbit IgG (H + L) AF Plus 488, Thermo Fisher Scientific, #A48282, Darmstadt, Germany) and DAPI (20 μg/ml) diluted in blocking buffer were added apically. Incubation was performed at RT for 1 h in the dark. To wash away unbound antibodies, cells were washed 5 times for 5 min each using PEMT. The membranes of the transwells were then separated from the well and embedded in the Mowiol mounting medium on an object slide for imaging using a Keyence BZ-X800 Fluorescence Microscope.

2.9. Statistical analysis

The presented results are expressed as mean values along with their corresponding standard deviations (SD). The SD was computed based on data collected from three independent experiments, except for the permeation results obtained with the tissue and the cell-based models, which were derived accordingly from four and ten independent

experiments, and for the immunostaining assay, for which 5 replicates were produced. Statistical analysis was carried out for all experimental data using a *t*-test, with significance determined for p-values lower than 0.05.

3. Results and discussion

3.1. Human lactobacilli CFS

The three CFS were obtained through a very straightforward downstream process that consists of two main steps: centrifugation of lactobacilli broth to isolate the supernatant and filtration to remove eventual residual cells and cell debris. CFS were employed in their liquid form and were characterized by both a typical yellowish color, due to the MRS broth components, and an acidic pH. The latter was found to range between 3.60 and 3.83, with BC5-CFS and BC12-CFS featuring the lower and the higher pH values, respectively. The low pH of the isolated CFS agreed with previously published results and was due to the metabolic activity of lactic acid bacteria, which tends to acidify the culture medium [21]. Since the pH can simultaneously affect both the nasal mucosa health and the absorption of molecules across the biological barrier, it is suggested to keep the pH of the formulation close to that of the administering site [22], that is 5.5–6.5 [23]. Consequently, the pH of CFS was adjusted to the value of 6, preventing mucosal damage and/or irritation and differences in drug permeation.

3.2. CFS influence on cell viability

The potential cytotoxic effect of different volume ratios of BC5-CFS, BC9-CFS, and BC12-CFS on the porcine primary cell model of the olfactory epithelium was verified after 24 h treatment and the results are shown in Fig. 1. According to ISO 10993–5:2009, chemicals are to be considered cytotoxic when they cause a decrease in cell viability below 70 %; therefore, as it comes clear from the graph, none of the considered samples were found cytotoxic at the tested conditions. This implies that neither the composition of the lactobacilli culture medium (MRS) nor the products of the probiotic metabolism negatively impact cell survival. Wanting to prove the role of the CFS as permeation enhancers and, at the same time, to employ the excipients at reduced concentrations, the intermediate volume ratio of 25 % was selected for the following studies, even though none of the tested volume ratios negatively affected cell viability.

3.3. CFS influence on osmolality

Similarly to the pH, even osmolality can affect the nasal mucosa [24]. Pujara and co-workers, for example, perfused sodium chloride solutions of increasing osmolalities through the rat nasal cavity and evaluated their potential for cell damage. The authors observed that hypotonic solutions induced cell swelling, with a consequent remarkable release of lactate dehydrogenase (LDH). Differently, isotonic and hypertonic solutions exerted little effect in terms of LDH release, but a 600 mOsm/kg solution determined cell shrinking. Moreover, they noted that the functional mucociliary system was most efficiently maintained at the nasal isosmotic value (280 mOsm/kg [24,25]. In this study, NaCl 0.9 % (v/v) was chosen as a diluent because of its being isosmotic, and the influence of 25 % (v/v) of either MRS or one of three tested CFS was evaluated. Table 2 shows that samples' osmolalities were comprised between 280 mOsm/kg and 370 mOsm/kg, therefore they matched the requirement for being administered in the nasal cavity: they featured osmolality values close to the physiological one and did not exceed 500 mOsm/kg [26]. These results further support the safety of the investigated CFS, because, apart from not being cytotoxic, they are expected to be non-irritating or harmful to the mucosa. Besides, it has been demonstrated that by altering the osmolarity of a formulation it is possible to increase drug absorption, as cell swelling and shrinking can alter the epithelium paracellular permeability. This was verified for both cell-free and cell-based *in vitro* studies [27–29]. Consequently, the gathered osmolality values guaranteed that tonicity would not influence the subsequent permeation studies.

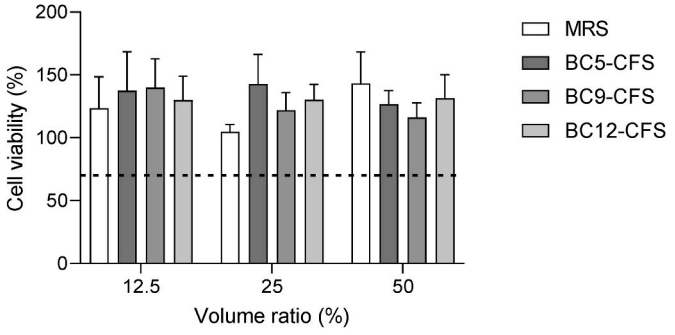

Fig. 1. CFS influence on porcine olfactory epithelial primary cells viability. Cell viability evaluation was performed after 24 h treatment with different volume ratios of either MRS or CFS. The black dotted line indicates 70 % cell viability. Data are reported as Mean + SD, n = 6.

3.4. CFS influence on fluorescein sodium salt permeability

When it comes to the initial stage of drug development, high-throughput screening of different compounds and formulations is highly convenient, but this is impractical with *in vivo* studies. Consequently, there is continuous research in the establishment of rapid and high-performance *in vitro* models to assess the permeability of compounds through the nasal epithelium and mucosa [30]. Therefore, in the present study, different *in vitro* models of the olfactory nasal mucosa were used to screen the selected CFS for their potential activity as enhancers towards FSS nose-to-brain permeation. Specifically, diffusion studies were performed across a cell-free, a tissue-based, and a cell-based model, thus gradually increasing the complexity and the informative level of the assay.

First, *in vitro* transport studies were carried out using the commercially available biomimetic membrane PermeaPad®. The latter features a dry film consisting of soybean phosphatidylcholine S-100, positioned between two low-retention layers of regenerated cellulose, functioning as support sheets. Upon hydration, the dry lipids swell and create a dense layer of vesicles interspersed in an aqueous environment, and this particular arrangement mimics cell organization within a tissue [31]. Fig. 2A depicts the permeation profiles of FSS across the PermeaPad® barrier when solubilized in normal saline solution alone (CTRL) or with 25 % (v/v) of either MRS or one of the investigated CFS. At first glance, the CTRL sample stands out as the only one featuring a lag time (t_{lag}), which was quantified in 7.69 ± 2.49 min, a short span but not negligible. Given that the thickness is a constant value (l), according to **Equation (3)** [32], the lag time is only dependent on the diffusion coefficient of the molecule (D).

$$t_{lag} = \frac{l^2}{6D} \qquad \text{Equation 3}$$

Table 2
Osmolality values of NaCl 0.9 % (w/v) in the absence (CTRL) and presence of 25 % (v/v) of either MRS or CFS. Data are reported as Mean ± SD, n = 3.

Sample	mOsm/kg	SD
CTRL	280.67	1.15
MRS	313.00	2.00
BC5-CFS	370.00	0.00
BC9-CFS	360.33	1.15
BC12-CFS	355.67	2.08

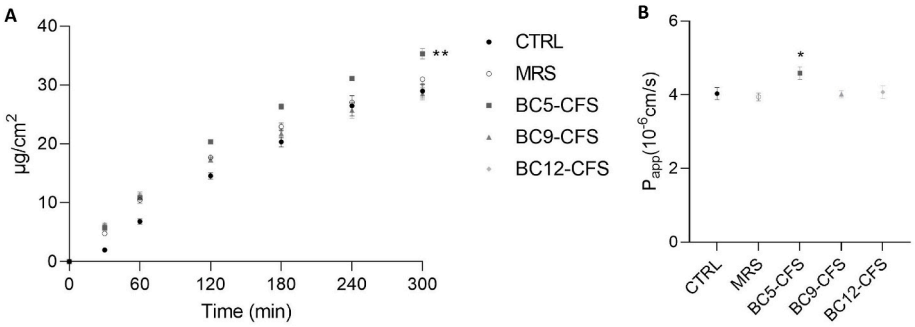

Fig. 2. Permeation study of fluorescein sodium salt across the cell-free model (PermeaPad® barrier) in the absence (CTRL) or presence of 25 % (v/v) of either the lactobacilli culture medium (MRS) or BC5/BC9/BC12-CFS. A) Permeation profiles. B) Apparent permeability coefficient (P_{app}). Data are reported as Mean ± SD, n = 3. Significance indicated by * = $p < 0.05$ compared to both CTRL and MRS; by ** = $p < 0.01$ compared to both CTRL and MRS.

This means that both CFS and MRS favored FSS diffusivity across the barrier. However, the mass permeated after 300 min was not significantly different between the tested samples (28.99 ± 1.16 µg/cm^2 CTRL; 30.98 ± 0.33 µg/cm^2 MRS; 28.52 ± 1.08 µg/cm^2 BC9-CFS; 30.07 ± 0.61 µg/cm^2 BC12-CFS), with the only exception of BC5-CFS, which enabled the permeation of the higher amount of the marker (35.31 ± 0.88 µg/cm^2). This is due to BC5-CFS's ability to greatly improve FSS flux across the barrier, quantified in 0.14 ± 0.01 µg/cm^{2}min, compared to all the other tested samples, which allowed FSS diffusion at a rate of 0.12 ± 0.01 µg/min each cm^2 of surface. This result has a relevant implication. Hence, considering the definition of the drug flux (J) according to **Equation (4)** [32]

$$J = -D\frac{dC}{dx} \qquad \text{Equation 4}$$

it is likely that BC5-CFS also influenced FSS solubility within the membrane, thus increasing the concentration gradient (dC/dx). In addition, the BC5-CFS effect on the marker flux ultimately resulted in an apparent permeability coefficient of 4.59 ± 0.17 10^{-6} cm/s, which was significantly increased compared to both the CTRL (4.03 ± 0.16 10^{-6} cm/s) and MRS (3.94 ± 0.11 10^{-6} cm/s) samples (Fig. 2B).

To perform diffusion studies across a tissue-based system, the porcine model was chosen because of its being considered suitable for nasal permeability studies [33]. As the tissue viability was not maintained because of its storage at −20 °C without the use of cryoprotectants, this model is characterized by membrane integrity [34] and a more complex architecture compared to the PermeaPad® barrier but, similarly to the cell-free model, it can only account for molecules' passive diffusion. Interestingly, when testing FSS permeation across the excised olfactory tissue, not only the CTRL but also the MRS-containing sample displayed a lag time, corresponding respectively to 17.34 ± 7.52 min and 20.41 ± 9.64 min (Fig. 3A). Therefore, it can be stated that, because any of the CFS-containing samples showed a lag time, it was the probiotic metabolism that made the difference in terms of diffusivity. Further, the permeation profiles of the CTRL and MRS samples almost overlapped, thus allowing for the diffusion of a similar amount of FSS: 45.11 ± 2.02 µg/cm^2 and 42.31 ± 3.40 µg/cm^2 in the absence and presence of the lactobacilli culture medium, respectively. Instead, the addition of 25 % (v/v) of any one of the tested CFS significantly increased the permeated mass compared to both reference samples, but the diffused FSS after 300 min did not differ between the three (52.40 ± 4.26 µg/cm^2 BC5-CFS; 50.51 ± 4.75 µg/cm^2 BC9-CFS; 52.33 ± 2.09 µg/cm^2 BC12-CFS). When it comes to the apparent permeability coefficient (Fig. 3B), compared to what was observed with the cell-free model, BC9-CFS (7.37 ± 0.37 10^{-6} cm/s) and BC12-CFS (7.81 ± 0.88 10^{-6} cm/s) showed a tendency to enhance FSS apparent permeability, but differences were deemed significant just with respect to the MRS sample (6.47 ± 0.54 10^{-6} cm/s). This means that the composition of the two CFS did not provide particular advantages compared to an FSS standard solution. Instead, the use of the CFS produced by BC5 demonstrated once more its enhancing properties, as it was able to increase FSS P_{app} from 6.88 ± 0.61 10^{-6} cm/s in the CTRL to 9.23 ± 0.89 10^{-6} cm/s. Again, probably this is the result of a dual effect: BC5-CFS might act on both the molecule diffusion coefficient and solubility in the membrane.

The third and last permeation model was the cell-based one. RPMI 2650 is the only immortalized cell line obtained from the nasal cavity of a human being and is regarded as the standard *in vitro* cell-based model to investigate nasal drug permeation [35,36], including the nose-to-brain route [37]. However, we thought that some of the features of the RPMI 2650 model did not fit the purpose of the present study. First of all, the permanent cell line was originally derived from the nasal septum, which belongs to the respiratory region of the nose rather than the olfactory one. Secondly, RPMI 2650 cells have a limited

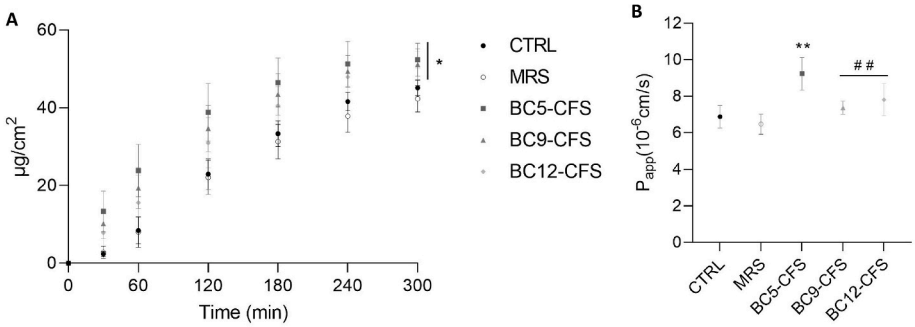

Fig. 3. Permeation study of fluorescein sodium salt across the tissue-based model (porcine olfactory mucosa) in the absence (CTRL) or presence of 25 % (v/v) of either the lactobacilli culture medium (MRS) or BC5/BC9/BC12-CFS. A) Permeation profiles. B) Apparent permeability coefficient (P_{app}). Data are reported as Mean ± SD, n = 4. Significance indicated by * = $p < 0.05$ between samples on the left side of the black line compared to both CTRL and MRS; by ** = $p < 0.01$ compared to both CTRL and MRS; by ## = $p < 0.01$ between the samples under the black line compared to MRS.

differentiative capacity and thus cannot reproduce the heterogeneous cell type composition of the olfactory mucosa [20]. Moreover, they tend to create a leaky multilayered barrier [20], which could make it difficult to point out the influence of CFS on the permeability of a model molecule such as FSS, which is supposed to permeate through the paracellular pathway. Consequently, we employed the porcine olfactory primary cell model that Ladel and colleagues have recently developed. It consists of a monolayer of porcine olfactory epithelial cells that differentiated over 21 days thereby producing a functional epithelial barrier, with secreted mucins and cilia [20]. Fig. 4A displays the permeation profiles across the cell-based model and the most striking difference compared to the aforementioned systems is that all tested samples exhibited a lag time. It must also be said that the lag time measured for the three CFS (78.16 ± 8.14 min BC5-CFS; 42.65 ± 4.94 min BC9-CFS; 55.15 ± 19.55 min BC12-CFS) was higher compared to both the CTRL (20.53 ± 6.35 min) and the MRS (10.51 ± 6.41 min) samples, suggesting that the lactobacilli metabolic products negatively impact the time required to reach the steady state. Nevertheless, only when FSS diffusion took place in the presence of the CFS, a greater increase in mass permeation was observed, as demonstrated by profiles featuring high slopes. As a result, both the mass permeated after 300 min (m) and flux (j) were remarkably higher in the presence of CFS (m = 23.99 ± 3.31 μg/cm^2 − j = 0.10 ± 0.02 μg/cm^{2}min BC5-CFS; m = 19.66 ± 2.45 μg/cm^2 − j = 0.07 ± 0.01 μg/cm^{2}min BC9-CFS; m = 17.81 ± 4.68 μg/cm^2 − j = 0.07 ± 0.02 μg/cm^{2}min BC12-CFS) compared to both reference samples (m = 9.20 ± 1.18 μg/cm^2 − j = 0.03 ± 0.01 μg/cm^{2}min CTRL; m = 12.78 ± 2.67 μg/cm^2 − j = 0.04 ± 0.01 μg/cm^{2}min MRS). Referring to **Equation (4)**, in this case, it is not clear whether the increase in the marker flux was the result of the CFS influence on diffusivity or concentration gradient, or both. What is evident is their permeation enhancer activity as demonstrated by P_{app} coefficients in Fig. 4B. The apparent permeability of FSS was greatly improved from 1.15 ± 0.18 10^{-6} cm/s and 1.45 ± 0.31 10^{-6} cm/s in the CTRL and MRS samples respectively, to 3.47 ± 0.52 10^{-6} cm/s, 2.68 ± 0.37 10^{-6} cm/s, and 2.42 ± 0.76 10^{-6} cm/s accordingly in BC5-CFS, BC9-CFS, and BC12-CFS. The graph also shows that MRS itself was able to significantly improve the P_{app} of the fluorescent marker, suggesting that there must be some inherent components of the culture medium bearing the ability to enhance small hydrophilic molecule permeation.

To gain a deeper understanding of the extent to which the investigated CFS improved FSS permeation, we calculated the enhancement ratio. The data presented in Fig. 5 highlight the predominant role of BC5-CFS as a permeation enhancer and they also prove the predictive power of the three *in vitro* models, as they ranked the same CFS as the best-performing enhancer. Besides, it must be noted that, when diffusion studies were performed across the cell-based model, also BC9-CFS and BC12-CFS acted as enhancers. Furthermore, it seems that the ER values of the CFS rise with the increase in the barrier system complexity. These

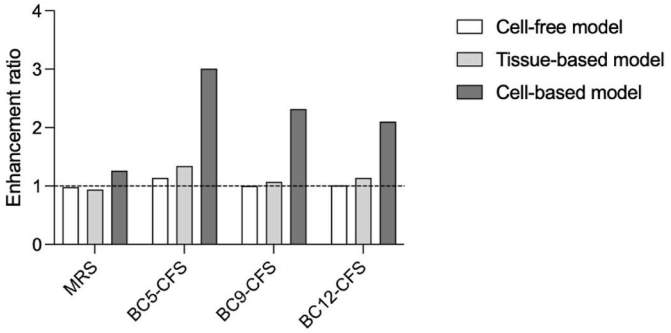

Fig. 5. Enhancement ratio (ER) of CFS and MRS when tested on the three *in vitro* barriers: cell-free model (PermePad® barrier), tissue-based model (excised porcine olfactory mucosa), and cell-based model (porcine olfactory epithelial primary cells). Only samples exhibiting ER > 1 (indicated by the black dotted line) are to be considered enhancers.

observations suggest that the three CFS might improve FSS diffusion because of a preferential interaction with some components of the tested barriers, such as lipids and proteins. Reasonably, the improvement in FSS permeability must be due to the composition of the CFS. Parolin and co-workers described the metabolites present in the cell-free supernatants of different human *Lactobacillus* strains, including those selected in the present study. Even though the CFS composition was strain-specific, the authors observed a common subset of molecules comprising amino acids, organic acids, monosaccharides, ketones, and alcohols [21]. Specifically, what stands out is the presence of some organic acids such as lactic acid, and orotate (mostly represented in BC5-CFS). Organic acids have been previously proven to function as enhancer molecules in transdermal drug delivery, and lactic acid was seen to outperform compared to other related substances [38], thus it might be possible that a similar role is played in nose-to-brain delivery as well. Alongside, in the case of the cell-based model, it cannot be excluded that, apart from paracellular diffusion, some sort of transcellular transport took place. Indeed, on the surface of olfactory epithelial cells different membrane-associated channel proteins have been identified. Aquaporins, for instance, are involved in the bidirectional transport of water, but small solutes and ions can also be transferred through this mechanism [39]. Moreover, amino acids, organic acids, and nucleosides contained in the CFS obtained from BC5, BC9, and BC12 [21] can be the substrates of different SLC (solute carrier) transporters [40].

The use of a small hydrophilic paracellular marker, such as fluorescein sodium salt, which is often exploited to evaluate the tightness and integrity of barriers [41], also allowed us to gather information regarding membrane suitability for nasal *in vitro* diffusion studies. Comparing the P_{app} of FSS across our barrier systems to that reported in the literature for the RPMI 2650 cell line, the only value that was

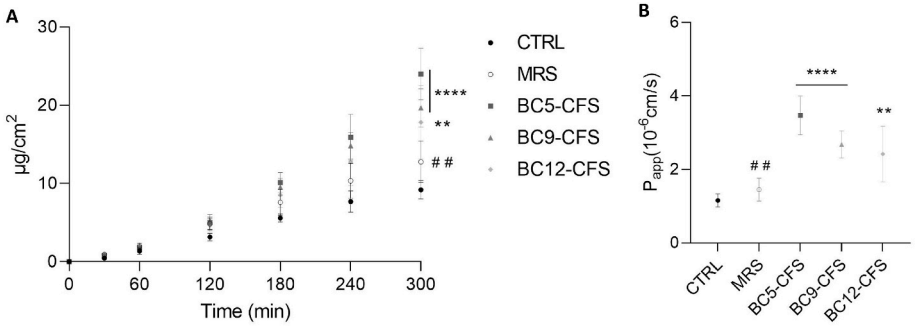

Fig. 4. Permeation study of fluorescein sodium salt across the cell-based model (porcine olfactory epithelial primary cell) in the absence (CTRL) or presence of 25 % (v/v) of either the lactobacilli culture medium (MRS) or BC5/BC9/BC12-CFS. A) Permeation profiles. B) Apparent permeability coefficient (P_{app}). Data are reported as Mean ± SD, n = 10. Significance indicated by **** = p < 0.0001 between samples on the left side of the black line (A) or under the black line (B) compared to both CTRL and MRS; by ** = p < 0.01 compared to both CTRL and MRS; by ## = p < 0.01 compared to CTRL.

deemed significantly different was that measured across the cell-based model Fig. 6. This is probably due to the primary nasal epithelial cells' tendency to develop an excessive number of tight junctions (TEER values measured 1753.42 ± 557.44 Ω cm^2) compared to both the excised tissue from which they were isolated (TEER values reported for the porcine mucosa 30–250 Ω cm^2 [42]) and the immortalized cell line (TEER values reported for RPMI2650 cell line 55–75 Ω cm^2 [20]). For this reason, combining studies on different barrier types might represent a more complete and reliable approach to assess the performance of molecules [33]. However, it must be said that the P_{app} measured for FSS across the primary cell model was closer ($p = 0.0136$) to that reported across the excised human mucosa (3.12 ± 1.99 10^{-6} cm/s [41]).

3.5. CFS influence on lipid membranes

We speculated that the increase in the P_{app} of FSS might be the result of an interaction between probiotic metabolites and phospholipid bilayers. Therefore, to better elucidate the mechanism of permeation enhancement operated by CFS, DSC analyses were performed on the excised porcine olfactory mucosa untreated (CTRL) and treated with 25 % (v/v) of MRS or one of the CFS under investigation. Fig. 7 shows that the CTRL sample was characterized by an endothermic peak at 71.06 °C, which is coherent with lipid transitions, that according to Corbo and co-workers should occur between 70 °C and 100 °C [43]. However, olfactory mucosa treatment with either MRS or one of CFS determined a shift in the endothermic peak to lower temperatures: 64.31 °C, 56.06 °C, 59.50 °C, and 58.80 °C for MRS, BC5-CFS, BC9-CFS, and BC12-CFS respectively. This suggests that lactobacilli's CFS can perturb the lipids within the nasal mucosa, and it is likely that this effect contributes to the increase in membrane permeability. Concerning the work of Parolin et al. [21], there are some molecules present in the CFS of BC5, BC9, and BC12 that catch the eye, in particular, butyrate (only present in BC5-CFS) and ethanol. The first belongs to the family of salts of fatty acids, which are known for their permeation-enhancing properties due to their ability to alter the lipid environment and cause membrane fluidization [44,45]. Ethanol, instead, features an established ability to increase membrane fluidity and pores formations, which has been exploited for example to increase transdermal absorption of drugs [38]. Therefore, these two elements might improve FSS permeation through their interaction with the lipid component of the three tested barriers.

3.6. CFS influence on tight junctions

FSS is a well-established marker of paracellular transport, therefore the observation of an improved permeability, particularly on the primary cell-based model, prompted us to investigate a potential involvement of CFS in tight junction modulation. To do so, olfactory primary cell monolayers were treated with either sodium chloride 0.9 % (CTRL), MRS, or the CFS for 5 h, and two data were acquired: the TEER values at the beginning and the end of the experiment, as well as the immunoreactivity against ZO-1, which is a polypeptide that connects tight junction proteins (i.e. occludin and claudin) to the cytoskeleton [46]. Fig. 8 shows the percentage of decrease in TEER between the starting and the end point of the analysis. Interestingly, the CTRL sample itself presents a 44.28 ± 13.72 % reduction, which is probably due to the change in the basolateral medium composition [47]; in fact, the primary culture medium was substituted with MEM without phenol red solely supplemented with 10 % FBS. Furthermore, the presence of MRS determined a significant decrease in TEER (65.33 ± 5.14 %) compared to the CTRL sample, which correlates with the enhancing effect observed on the cell-based model and the influence on lipids' endothermic peak. Most notably, the influence on TEER was even greater when primary cells were treated with CFS and, in agreement with the permeation and DSC studies, BC5-CFS demonstrated the highest influence on TEER (81.07 ± 3.66 %).

The measurement of TEER reduction is often employed as a screening parameter to investigate tight junction modulation ability by permeation enhancers [44], therefore we expected to observe a

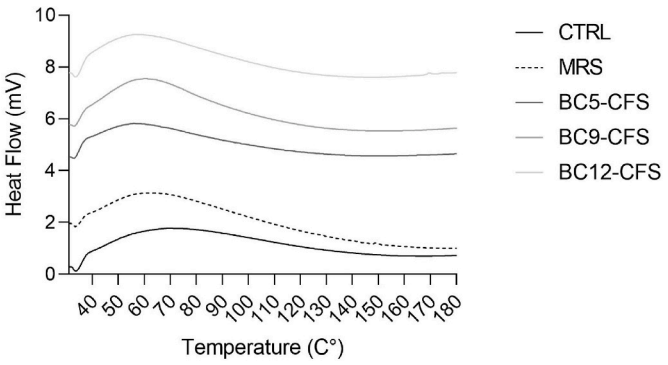

Fig. 7. Differential scanning calorimetry curves of the excised porcine olfatoy mucosa untreated (CTRL) and treated with 25 %(v/v) or MRS or BC5/BC9/BC12-CFS.

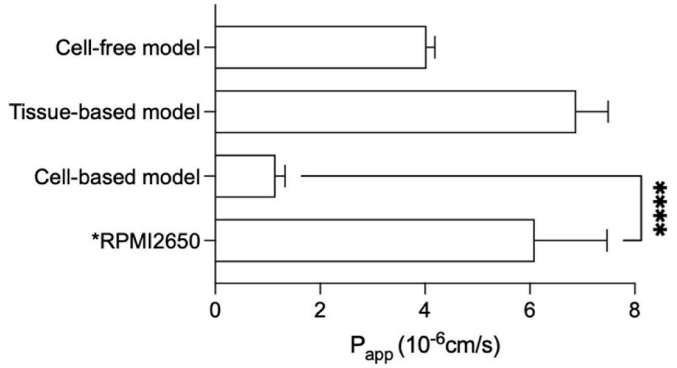

Fig. 6. Apparent permeability coefficients (P_{app}) of fluorescein sodium salt through the cell-free (PermeaPad® barrier), tissue based (excised porcine olfactory mucosa), and cell-based (porcine olfactory primary epithelial cell) models compared to P_{app} calculated by [41] across the RPMI2650 cell line. Data are reported as Mean ± SD, n ≥ 3. Statistical differences between samples are indicated by **** = $p < 0.0001$.

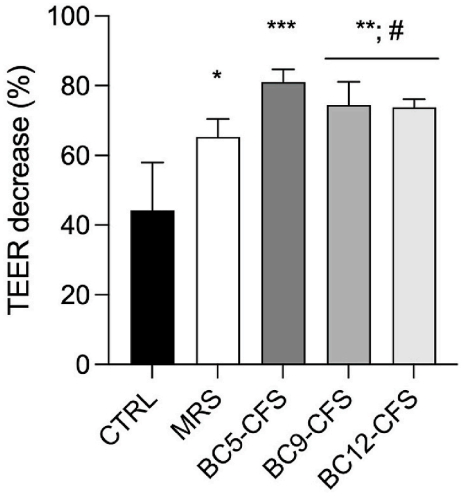

Fig. 8. Olfactory epithelial primary cells' percentage of TEER decrease after 5 h treatment with 25 % (v/v) of either MRS or CFS. Data are reported as Mean ± SD, n = 5. Significance indicated by * = $p < 0.05$ compared to CTRL; by # = $p < 0.05$ between samples under the black line compared to MRS; by ** = $p < 0.01$ between samples under the black line compared to CTRL; by *** = $p < 0.001$ compared to both CTRL and MRS.

correlation between TEER decrease and ZO-1 immunostaining distribution. However, as is pointed out in Fig. 9, any difference could be highlighted neither in terms of tight junctions' staining pattern (Fig. 9A–E) nor in fluorescence intensity (Fig. 9F). The absence of an evident disruption of cell-cell connections might indicate that CFS influence tight junctions' activity rather than their localization. This outcome is further supported by the work of Chen-Quay et al., who demonstrated the ability of PGPC (1-palmitoyl-2-glutaroyl-*sn*-glycero-3-phosphocholine) to cause a reduction in TEER values without affecting the structural integrity of tight junctions in EpiAirway tissues [48]. The authors suggested the possibility for their candidate lipid to interact with the lipid rafts where tight junctions' proteins localize, thereby influencing both membrane permeability and electrical resistance [48].

4. Conclusions

Based on the current information, this is the first attempt to demonstrate the applicability of postbiotics, like CFS, as permeation enhancers in nose-to-brain drug delivery. Moreover, this innovative approach might be of particular interest for the development of more sustainable and less pollutant pharmaceuticals. Indeed, CFS are obtained from naturally occurring and health-promoting human lactobacilli through a simple, easily scalable, and green (extraction using toxic and harmful solvents is not required) procedure. Besides, as CFS are frequently discarded by many food and pharmaceutical industries [49], their use would contribute to the reduction of waste and even the microbial cells could be used to produce probiotic-containing delivery systems [50]. Among the screened CFS in the study, BC5-CFS outperformed as a permeation enhancer and the robustness of the result is supported by the use of three *in vitro* models of the olfactory epithelium. The fact that different barriers highlighted diverse behaviors (the presence of lag time as well as BC9-CFS and BC12-CFS's ability to improve FSS permeability across the cell-based model) suggests that each model should be preferred depending on the scientific need. Specifically, the PermeaPad® barrier is surely a promising tool for a sustainable, less time-consuming, and cost-effective screening of enabling formulations. However, when selecting those excipients and/or drugs to be further optimized during the late stages of the pharmaceutical development process, it might be also useful to rely on more complete models, i.e., cell-based models. The mixture of metabolites present in BC5-CFS likely increases FSS permeation by perturbing the lipid environment within the tested barriers which, in the case of OEPC, seems to exert an effect on tight junctions, as demonstrated by the decrease in TEER values. Nonetheless, this outcome does not affect either barrier integrity or cell viability. Hopefully, these results will encourage the introduction of BC5-CFS as an innovative natural and green excipient in the field of nose-to-brain delivery of small hydrophilic molecules. Nonetheless, further studies should be performed to investigate the CFS' minimal effective concentration as well as BC5-CFS applicability in nasal formulations intended for the delivery of drugs with different physicochemical properties compared to FSS.

Funding

This research was funded by the Deutsche Forschungsgemeinschaft ("OlfacMuc" grant No ZI-1143/HU441).

CRediT authorship contribution statement

Elisa Corazza: Writing – original draft, Validation, Methodology, Investigation, Formal analysis, Data curation. **Janik Martin:** Writing – original draft, Validation, Methodology, Investigation, Formal analysis, Data curation. **Barbara Giordani:** Writing – review & editing, Methodology. **Beatrice Vitali:** Writing – review & editing, Supervision, Resources, Conceptualization. **Martina Rossi:** Resources, Methodology. **Angela Abruzzo:** Writing – review & editing, Supervision. **Federica Bigucci:** Writing – review & editing, Supervision. **Teresa Cerchiara:** Writing – review & editing, Supervision. **Massimiliano Pio di Cagno:** Writing – review & editing, Validation. **Barbara Luppi:** Writing – review & editing, Supervision, Resources, Conceptualization. **Katharina Schindowski:** Writing – review & editing, Supervision, Resources, Conceptualization.

Declaration of competing interest

The authors declare that they have no known competing financial interests or personal relationships that could have appeared to influence the work reported in this paper.

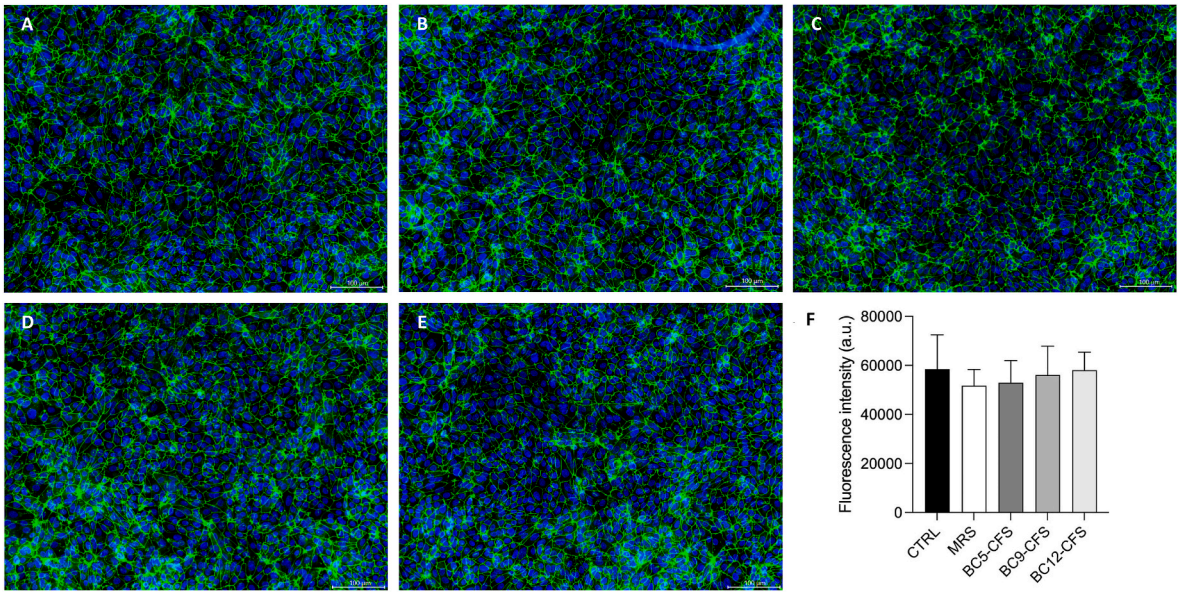

Fig. 9. Influence of CFS on tight junction integrity. A – E) Staining of the zonula occludens marker ZO-1 in olfactory epithelial primary cells treated for 5 h with either sodium chloride (A), MRS (B), BC5-CFS (C), BC9-CFS (D), or BC12-CFS (E). F) Fluorescence quantification; data are reported as Mean ± SD, n = 5.

Data availability

Data will be made available on request.

Acknowledgements

The authors would like to thank PHABIOC GmbH for providing the PermeaPad® barriers and Rebecca Rittersberger for her technical support. The authors wish also to express their thankfulness to the Center for Applied Biomedical Research (CRBA), University of Bologna, for allowing us to access its spaces and to use innovative tools essential for our research.

References

[1] H.D.O. Souza, R.D.S. Costa, G.R. Quadra, M.A.D.S. Fernandez, Pharmaceutical pollution and sustainable development goals: going the right way? Sustain. Chem. Pharm. 21 (2021) 100428 https://doi.org/10.1016/j.scp.2021.100428.
[2] N. Puhlmann, R. Vidaurre, K. Kümmerer, Designing greener active pharmaceutical ingredients: Insights from pharmaceutical industry into drug discovery and development, Eur. J. Pharm. Sci. 192 (2024) 106614, https://doi.org/10.1016/j.ejps.2023.106614.
[3] L.A.L. Silvério, J.C. Coco, L.M.D. Macedo, É.M.D. Santos, A.C. Sueiro, J.A. Ataide, G.D. Tavares, A.C. Paiva-Santos, P.G. Mazzola, Natural product-based excipients for topical green formulations, Sustain. Chem. Pharm. 33 (2023) 101111, https://doi.org/10.1016/j.scp.2023.101111.
[4] P. Thorakkattu, A.C. Khanashyam, K. Shah, K.S. Babu, A.S. Mundanat, A. Deliephan, G.S. Deokar, C. Santivarangkna, N.P. Nirmal, Postbiotics: current Trends in food and pharmaceutical industry, Foods 11 (2022) 3094, https://doi.org/10.3390/foods11193094.
[5] T. Teame, A. Wang, M. Xie, Z. Zhang, Y. Yang, Q. Ding, C. Gao, R.E. Olsen, C. Ran, Z. Zhou, Paraprobiotics and postbiotics of probiotic lactobacilli, their positive effects on the Host and action mechanisms: a review, Front. Nutr. 7 (2020) 570344, https://doi.org/10.3389/fnut.2020.570344.
[6] C. Liu, N. Ma, Y. Feng, M. Zhou, H. Li, X. Zhang, X. Ma, From probiotics to postbiotics: Concepts and applications, Anim. Res. One Health 1 (2023) 92–114, https://doi.org/10.1002/aro2.7.
[7] C. Carriço, H.M. Ribeiro, J. Marto, Converting cork by-products to ecofriendly cork bioactive ingredients: novel pharmaceutical and cosmetics applications, Ind. Crops Prod. 125 (2018) 72–84, https://doi.org/10.1016/j.indcrop.2018.08.092.
[8] M. Duarte, A.L. Oliveira, C. Oliveira, M. Pintado, A. Amaro, A.R. Madureira, Current postbiotics in the cosmetic market—an update and development opportunities, Appl. Microbiol. Biotechnol. 106 (2022) 5879–5891, https://doi.org/10.1007/s00253-022-12116-5.
[9] S. Madden, E. Carrazana, A.L. Rabinowicz, Optimizing absorption for intranasal delivery of drugs targeting the central Nervous system using Alkylsaccharide permeation enhancers, Pharmaceutics 15 (2023) 2119, https://doi.org/10.3390/pharmaceutics15082119.
[10] A. Lofts, F. Abu-Hijleh, N. Rigg, R.K. Mishra, T. Hoare, Using the intranasal route to administer drugs to treat neurological and Psychiatric Illnesses: Rationale, Successes, and Future needs, CNS Drugs 36 (2022) 739–770, https://doi.org/10.1007/s40263-022-00930-4.
[11] S. Grassin-Delyle, A. Buenestado, E. Naline, C. Faisy, S. Blouquit-Laye, L.-J. Couderc, M. Le Guen, M. Fischler, P. Devillier, Intranasal drug delivery: an efficient and non-invasive route for systemic administration, Pharmacol. Ther. 134 (2012) 366–379, https://doi.org/10.1016/j.pharmthera.2012.03.003.
[12] W. Yang, M. Lipert, R. Nofsinger, Current screening, design, and delivery approaches to address low permeability of chemically synthesized modalities in drug discovery and early clinical development, Drug Discov. Today 28 (2023) 103685, https://doi.org/10.1016/j.drudis.2023.103685.
[13] D.A. Volpe, Application of method suitability for drug permeability Classification, AAPS J. 12 (2010) 670–678, https://doi.org/10.1208/s12248-010-9227-8.
[14] A. Haasbroek-Pheiffer, S. Van Niekerk, F. Van Der Kooy, T. Cloete, J. Steenekamp, J. Hamman, *In vitro* and *ex vivo* experimental models for evaluation of intranasal systemic drug delivery as well as direct nose-to-brain drug delivery, Biopharm. Drug Dispos. 44 (2023) 94–112, https://doi.org/10.1002/bdd.2348.
[15] P. Henriques, J. Bicker, S. Silva, S. Doktorovová, A. Fortuna, Nasal-PAMPA: a novel non-cell-based high throughput screening assay for prediction of nasal drug permeability, Int. J. Pharm. 643 (2023) 123252, https://doi.org/10.1016/j.ijpharm.2023.123252.
[16] I.Y. Wu, S. Bala, N. Škalko-Basnet, M.P. di Cagno, Interpreting non-linear drug diffusion data: utilizing Korsmeyer-Peppas model to study drug release from liposomes, Eur. J. Pharm. Sci. 138 (2019) 105026, https://doi.org/10.1016/j.ejps.2019.105026.
[17] E.J. Carrasco-Correa, J. Ruiz-Allica, J.F. Rodríguez-Fernández, M. Miró, Human artificial membranes in (bio)analytical science: potential for in vitro prediction of intestinal absorption-A review, TrAC Trends Anal. Chem. 145 (2021) 116446, https://doi.org/10.1016/j.trac.2021.116446.
[18] E. Corazza, A. Abruzzo, B. Giordani, T. Cerchiara, F. Bigucci, B. Vitali, M.P. di Cagno, B. Luppi, Human Lactobacillus biosurfactants as natural excipients for nasal drug delivery of hydrocortisone, Pharmaceutics 14 (2022) 524, https://doi.org/10.3390/pharmaceutics14030524.
[19] C. Parolin, A. Abruzzo, B. Giordani, J.C. Oliver, A. Marangoni, B. Luppi, B. Vitali, Anti-Candida activity of Hyaluronic acid combined with Lactobacillus crispatus Lyophilised supernatant: a new Antifungal strategy, Antibiotics 10 (2021) 628, https://doi.org/10.3390/antibiotics10060628.
[20] S. Ladel, P. Schlossbauer, J. Flamm, H. Luksch, B. Mizaikoff, K. Schindowski, Improved in vitro model for intranasal mucosal drug delivery: primary olfactory and respiratory epithelial cells compared with the permanent nasal cell line RPMI 2650, Pharmaceutics 11 (2019) 367, https://doi.org/10.3390/pharmaceutics11080367.
[21] C. Parolin, A. Marangoni, L. Laghi, C. Foschi, R.A. Ñahui Palomino, N. Calonghi, R. Cevenini, B. Vitali, Isolation of vaginal lactobacilli and Characterization of anti-Candida activity, PLoS One 10 (2015) e0131220, https://doi.org/10.1371/journal.pone.0131220.
[22] A. Javia, G. Kore, A. Misra, Polymers in nasal drug delivery: an overview, in: Applications of Polymers in Drug Delivery, Elsevier, 2021, pp. 305–332, https://doi.org/10.1016/B978-0-12-819659-5.00011-2.
[23] M. Cirri, F. Maestrelli, G. Nerli, N. Mennini, M. D'Ambrosio, C. Luceri, P.A. Mura, Development of a Cyclodextrin-based Mucoadhesive-Thermosensitive in situ gel for Clonazepam intranasal delivery, Pharmaceutics 13 (2021) 969, https://doi.org/10.3390/pharmaceutics13070969.
[24] C. Campbell, B.H. Morimoto, D. Nenciu, A.W. Fox, Drug development of intranasally delivered peptides, Ther. Deliv. 3 (2012) 557–568, https://doi.org/10.4155/tde.12.12.
[25] C.P. Pujara, Z. Shao, M.R. Duncan, A.K. Mitra, Effects of formulation variables on nasal epithelial cell integrity: Biochemical evaluations, Int. J. Pharm. 114 (1995) 197–203, https://doi.org/10.1016/0378-5173(94)00238-Z.
[26] C. Bitter, K. Suter-Zimmermann, C. Surbera, Nasal drug delivery in humans, in: C. Surber, P. Elsner, M.A. Farage (Eds.), Current Problems in Dermatology, KARGER, Basel, 2011, pp. 20–35, https://doi.org/10.1159/000321044.
[27] C. Dufes, J.-C. Olivier, F. Gaillard, A. Gaillard, W. Couet, J.-M. Muller, Brain delivery of vasoactive intestinal peptide (VIP) following nasal administration to rats, Int. J. Pharm. 255 (2003) 87–97, https://doi.org/10.1016/S0378-5173(03)00039-5.
[28] J.B. Eriksen, H. Barakat, B. Luppi, M. Brandl, A. Bauer-Brandl, Modulation of paracellular-like drug transport across an artificial biomimetic barrier by Osmotic Stress-induced liposome shrinking, Pharmaceutics 14 (2022) 721, https://doi.org/10.3390/pharmaceutics14040721.
[29] J.-C. Olivier, M. Djilani, S. Fahmy, W. Couet, In situ nasal absorption of midazolam in rats, Int. J. Pharm. 213 (2001) 187–192, https://doi.org/10.1016/S0378-5173(00)00668-2.
[30] L.-A. Barlang, K. Weinbender, O.M. Merkel, A. Popp, Characterization of critical parameters using an air–liquid interface model with RPMI 2650 cells for permeability studies of small molecules, Drug Deliv. Transl. Res. (2023), https://doi.org/10.1007/s13346-023-01474-w.
[31] P. Berben, A. Bauer-Brandl, M. Brandl, B. Faller, G.E. Flaten, A.-C. Jacobsen, J. Brouwers, P. Augustijns, Drug permeability profiling using cell-free permeation tools: overview and applications, Eur. J. Pharm. Sci. 119 (2018) 219–233, https://doi.org/10.1016/j.ejps.2018.04.016.
[32] D. Selzer, M.M.A. Abdel-Mottaleb, T. Hahn, U.F. Schaefer, D. Neumann, Finite and infinite dosing: Difficulties in measurements, evaluations and predictions, Adv. Drug Deliv. Rev. 65 (2013) 278–294, https://doi.org/10.1016/j.addr.2012.06.010.
[33] A. Sosnik, Tissue-based in vitro and ex vivo models for nasal permeability studies, in: Concepts and Models for Drug Permeability Studies, Elsevier, 2016, pp. 237–254, https://doi.org/10.1016/B978-0-08-100094-6.00014-6.
[34] J.A. Nicolazzo, B.L. Reed, B.C. Finnin, The effect of various in vitro conditions on the permeability Characteristics of the Buccal mucosa, J. Pharm. Sci. 92 (2003) 2399–2410, https://doi.org/10.1002/jps.10505.
[35] W. Gerber, H. Svitina, D. Steyn, B. Peterson, A. Kotzé, C. Weldon, J.H. Hamman, Comparison of RPMI 2650 cell layers and excised sheep nasal epithelial tissues in terms of nasal drug delivery and immunocytochemistry properties, J. Pharmacol. Toxicol. Methods 113 (2022) 107131, https://doi.org/10.1016/j.vascn.2021.107131.
[36] V.S.S. Gonçalves, A.A. Matias, J. Poejo, A.T. Serra, C.M.M. Duarte, Application of RPMI 2650 as a cell model to evaluate solid formulations for intranasal delivery of drugs, Int. J. Pharm. 515 (2016) 1–10, https://doi.org/10.1016/j.ijpharm.2016.09.086.
[37] L. Deruyver, C. Rigaut, A. Gomez-Perez, P. Lambert, B. Haut, J. Goole, In vitro evaluation of Paliperidone palmitate loaded Cubosomes effective for nasal-to-brain delivery, Int. J. Nanomed. 18 (2023) 1085–1106, https://doi.org/10.2147/IJN.S397650.
[38] C. Ren, L. Fang, T. Li, M. Wang, L. Zhao, Z. He, Effect of permeation enhancers and organic acids on the skin permeation of indapamide, Int. J. Pharm. 350 (2008) 43–47, https://doi.org/10.1016/j.ijpharm.2007.08.020.
[39] S. Gänger, K. Schindowski, Tailoring formulations for intranasal nose-to-brain delivery: a review on architecture, Physico-Chemical Characteristics and mucociliary clearance of the nasal olfactory mucosa, Pharmaceutics 10 (2018) 116, https://doi.org/10.3390/pharmaceutics10030116.
[40] U. Anand, A. Parikh, M.C. Ugwu, R.U. Agu, Drug transporters in the nasal epithelium: an overview of strategies in targeted drug delivery, Future Med. Chem. 6 (2014) 1381–1397, https://doi.org/10.4155/fmc.14.77.
[41] A. Wengst, S. Reichl, RPMI 2650 epithelial model and three-dimensional reconstructed human nasal mucosa as in vitro models for nasal permeation studies, Eur. J. Pharm. Biopharm. 74 (2010) 290–297, https://doi.org/10.1016/j.ejpb.2009.08.008.

[42] C. Wadell, E. Björk, O. Camber, Nasal drug delivery – evaluation of an in vitro model using porcine nasal mucosa, Eur. J. Pharm. Sci. 7 (1999) 197–206, https://doi.org/10.1016/S0928-0987(98)00023-2.
[43] D.C. Corbo, J.-C. Liu, Y.W. Chien, Characterization of the barrier properties of mucosal membranes, J. Pharm. Sci. 79 (1990) 202–206, https://doi.org/10.1002/jps.2600790304.
[44] M. Ghadiri, F. Canney, C. Pacciana, G. Colombo, P.M. Young, D. Traini, The use of fatty acids as absorption enhancer for pulmonary drug delivery, Int. J. Pharm. 541 (2018) 93–100, https://doi.org/10.1016/j.ijpharm.2018.02.027.
[45] A. Katdare, S. Thakkar, S. Dhepale, D. Khunt, M. Misra, Fatty acids as essential adjuvants to treat various ailments and their role in drug delivery: a review, Nutrition 65 (2019) 138–157, https://doi.org/10.1016/j.nut.2019.03.008.
[46] H.J. Lemmer, J.H. Hamman, Paracellular drug absorption enhancement through tight junction modulation, Expet Opin. Drug Deliv. 10 (2013) 103–114, https://doi.org/10.1517/17425247.2013.745509.
[47] B. Srinivasan, A.R. Kolli, M.B. Esch, H.E. Abaci, M.L. Shuler, J.J. Hickman, TEER measurement Techniques for in vitro barrier model systems, SLAS Technol 20 (2015) 107–126, https://doi.org/10.1177/2211068214561025.
[48] S. Chen-Quay, K.T. Eiting, A.W.-A. Li, N. Lamharzi, S.C. Quay, Identification of tight junction modulating lipids, J. Pharm. Sci. 98 (2009) 606–619, https://doi.org/10.1002/jps.21462.
[49] P. Raknam, N. Balekar, R. Teanpaisan, T. Amnuaikit, Thermoresponsive sol–gel containing probiotic's cell free supernatant for dental caries prophylaxis, J. Oral Microbiol. 14 (2022) 2012390, https://doi.org/10.1080/20002297.2021.2012390.
[50] B. Vitali, A. Abruzzo, C. Parolin, R.A.Ñ. Palomino, F. Dalena, F. Bigucci, T. Cerchiara, B. Luppi, Association of Lactobacillus crispatus with fructo-oligosaccharides and ascorbic acid in hydroxypropyl methylcellulose vaginal insert, Carbohydr. Polym. 136 (2016) 1161–1169, https://doi.org/10.1016/j.carbpol.2015.10.035.